

## Surface of a spin-polarized electron gas

R. L. Kautz\*

*Francis Bitter National Magnet Laboratory,<sup>†</sup> Massachusetts Institute of Technology, Cambridge, Massachusetts 02139  
and Magnetic Theory Group, Department of Physics, Northwestern University, Evanston, Illinois 60201<sup>‡</sup>*

Brian B. Schwartz

*Francis Bitter National Magnet Laboratory,<sup>†</sup> Massachusetts Institute of Technology, Cambridge, Massachusetts 02139  
(Received 29 March 1976)*

The surface of a spin-polarized electron gas is used to model the conduction electrons at the surface of both a simple metal in a magnetic field and ferromagnetic gadolinium. A self-consistent calculation based on the Hohenberg-Kohn-Sham density-functional formalism obtains the densities of majority and minority-spin electrons at the surface. For a simple metal, we calculate the position-dependent susceptibility which describes the response of the surface to a uniform magnetic field. For gadolinium, we obtain the change in work function, surface magnetization, and surface energy between the paramagnetic and saturated ferromagnetic states.

### I. INTRODUCTION

The surface of a paramagnetic electron gas has long served as a model for the conduction electrons at the surface of a simple metal. This jellium model results when the metal ions are replaced with a uniform positive charge density which ends abruptly at the surface plane. The basic validity of the jellium model has been demonstrated by Lang and Kohn who derive values for the work function and surface energy of the alkali metals in good agreement with experiment.<sup>1,2</sup>

The present work considers the surfaces of two metallic systems which can be modeled by a spin-polarized electron gas, the conduction electrons of a simple metal in a uniform magnetic field and the conduction electrons of ferromagnetic gadolinium. The models adopted for these two systems differ from the jellium model only by the presence of a polarizing field  $\vec{J}$ , which introduces a magnetic term  $-\vec{\sigma} \cdot \vec{J}$  into the Hamiltonian and lowers (raises) the energy of electrons with spin  $\vec{\sigma}$  parallel (antiparallel) to  $\vec{J}$ . For a simple metal in a uniform magnetic field,  $\vec{J}$  is a constant field proportional to the magnetic field  $\vec{J} = \mu_B \vec{B}$ . Treating this system in the limit of small  $B$ , we obtain an accurate result for the surface susceptibility of an alkali metal. For ferromagnetic Gd, spin polarization results from an exchange interaction between the conduction electrons and the localized  $4f$  moments. From the viewpoint of the conduction electrons this exchange interaction is conveniently represented by an exchange field, mathematically equivalent to a magnetic field, having a magnitude roughly proportional to the magnetization of the  $4f$  electrons. To model the surface of Gd we choose a  $\vec{J}$  which is constant in the bulk and falls abruptly to zero at the surface, thus simulating

the sudden disappearance of  $4f$  magnetization at the surface. While the resulting model is highly simplified in that it neglects both the  $d$  character of the gadolinium conduction band and inhomogeneities in the bulk exchange field, it otherwise includes the essential physical elements. Estimates are obtained for the surface magnetization of the conduction electrons, the work function, and the surface energy of paramagnetic and ferromagnetic Gd.

The two spin-polarized surface models considered are simple and yet physically interesting. The solutions obtained are accurate self-consistent solutions based on the density-functional formalism of Hohenberg and Kohn<sup>3</sup> and Kohn and Sham<sup>4</sup> as extended to the spin-polarized case by von Barth and Hedin<sup>5</sup> and Rajagopal and Callaway.<sup>6</sup> These solutions represent the first self-consistent calculation of the surface magnetization of a metallic system.

By neglecting the periodic potential a jellium model omits band-structure effects entirely. For the alkali metals, in which the periodic potential can be replaced by a weak pseudopotential, the jellium approximation is justifiable. In the case of gadolinium, which has a complex band structure, neglect of the periodic potential is clearly an oversimplification. The jellium approximation has been adopted here for reasons of calculational simplicity. In principle, density-functional calculations could be extended to include the periodic potential, just as the work of Lang and Kohn<sup>1</sup> has been extended by Appelbaum and Hamann.<sup>7</sup> With this in mind, we have chosen to explore the spin-dependent density-functional formalism in some detail. In particular, we compare accurate self-consistent solutions to the surface problem based on the Hartree-Fock (HF) and random-phase-ap-

proximation (RPA) energy functionals.

A number of recent calculations of both the surface susceptibility of a paramagnetic metal<sup>8-10</sup> and the surface magnetization of a ferromagnetic metal<sup>11-13</sup> have been based on the Hubbard model. The advantage of the Hubbard model over a jellium model is that it introduces band-structure effects in a simple fashion. The disadvantage is that hopping integrals and intra-atomic Coulomb integrals are difficult to calculate for the surface layer. Although crude estimates for these quantities can be obtained from renormalized-atom theory,<sup>11, 12</sup> they have usually been taken as free parameters. Because the magnetic nature of the surface solution is quite sensitive to the intra-atomic Coulomb integral,<sup>12, 13</sup> it has proven difficult to draw definite conclusions about real systems from the Hubbard model. While our results for ferromagnetic Gd are also tentative, the physical origin of the model is clear and the solution contains no free parameters.

Because a surface solution implies a bulk solution, we begin with a discussion of the uniform spin-polarized electron gas, presenting in Sec. II both the HF and RPA solutions. In Sec. III we discuss the spin-polarized version of the density-functional formalism. Equations for the surface problem are developed in Sec. IV and solutions for the two surface models are discussed in Sec. V.

## II. UNIFORM SPIN-POLARIZED ELECTRON GAS

Consider a gas of electrons at zero temperature in the presence of a uniform neutralizing charge density and a uniform polarizing field. The spin-polarized electron gas is characterized by two parameters, the density of electrons  $n = 3/4\pi(a_0 r_s)^3$  and the strength of the polarizing field  $J$ . The Hamiltonian for the spin-polarized gas is<sup>14</sup>

$$H = \sum_{k\sigma} \left( \frac{\hbar^2 k^2}{2m} - \sigma J \right) c_{k\sigma}^\dagger c_{k\sigma} + \frac{1}{2\Omega} \sum_{\substack{k, k', q \\ \sigma\sigma'}} \frac{4\pi e^2}{q^2} c_{k+\sigma q}^\dagger c_{k'-\sigma q}^\dagger c_{k'\sigma'} c_{k\sigma}, \quad (2.1)$$

where the direction of spin quantization has been chosen such that the  $\sigma = +$  and  $\sigma = -$  states are parallel and antiparallel to  $\vec{J}$ .

The spin-polarized gas has not previously been treated as a many-body system except in the limit of small polarizing fields. A number of authors have, however, investigated an electron gas that is assumed to be polarized in the absence of a polarizing field and much of this work can be applied to the system considered here.

### A. Hartree-Fock approximation

For a uniform electron gas, the HF wave function is a Slater determinant of single-particle states having definite momentum  $k$  and spin  $\sigma$ . The ground state is constructed by filling the plane-wave states of lowest energy. For the ground state all spin  $\sigma$  states with momentum less than  $k_{F\sigma} = (6\pi^2 n_\sigma)^{1/3}$  will be occupied; given that the density of spin  $\sigma$  electrons is  $n_\sigma$ . The energy per particle of the ground state can be written in terms of  $r_s$ ,  $J$ , and the relative magnetization  $\zeta = (n_+ - n_-)/n$  as

$$\epsilon_{\text{HF}} = \epsilon_k + \epsilon_x + \epsilon_m, \quad (2.2)$$

$$\epsilon_k = \frac{e^2}{a_0} \frac{3^{7/3} \pi^{2/3}}{2^{10/3} 5} [(1 + \zeta)^{5/3} + (1 - \zeta)^{5/3}] \frac{1}{r_s^2}, \quad (2.3)$$

$$\epsilon_x = -\frac{e^2}{a_0} \frac{3^{5/3}}{2^{11/3} \pi^{2/3}} [(1 + \zeta)^{4/3} + (1 - \zeta)^{4/3}] \frac{1}{r_s}, \quad (2.4)$$

$$\epsilon_m = -\zeta J, \quad (2.5)$$

where  $\epsilon_k$ ,  $\epsilon_x$ , and  $\epsilon_m$  are the kinetic, exchange, and magnetic energies, respectively. Except for the added magnetic term, this result is the same as that of Bloch.<sup>15</sup>

The relative magnetization of the ground state for a given  $r_s$  and  $J$  is determined by choosing  $\zeta$  to minimize the total energy. Requiring that  $d\epsilon_{\text{HF}}/d\zeta = 0$  yields

$$J = \frac{e^2}{a_0} \frac{3^{4/3} \pi^{2/3}}{2^{10/3}} [(1 + \zeta)^{2/3} - (1 - \zeta)^{2/3}] \frac{1}{r_s^2} - \frac{e^2}{a_0} \frac{3^{2/3}}{2^{5/3} \pi^{2/3}} [(1 + \zeta)^{1/3} - (1 - \zeta)^{1/3}] \frac{1}{r_s}. \quad (2.6)$$

The value of  $\zeta$  which satisfies this equation does not always minimize the total energy. The actual dependence of  $\zeta$  on  $r_s$  and  $J$  is shown in Fig. 1. For  $r_s > 5.45$ , the ground state proves to be the  $\zeta = 1$  state for all  $J$ . For  $r_s < 5.45$ , the magnetization follows Eq. (2.6) up to some critical polarizing field and then switches suddenly from some partial magnetization ( $\zeta < 1$ ) to full magnetization ( $\zeta = 1$ ).

The spontaneous ferromagnetism of the HF gas for  $r_s > 5.45$  is explained by the fact that in the HF approximation electron correlation results entirely from the Pauli exclusion principle and only spin-parallel electrons are correlated. The interaction energy of two electrons is thus less if the electrons are of parallel spin than if they are of opposite spin. As a result, the interaction energy of the ferromagnetic state is lower than that of the paramagnetic state. Because the alignment of spins requires the transfer of electrons to high momentum states, the kinetic energy increases with polarization. When  $r_s$  is small and  $\epsilon_k \gg |\epsilon_x|$  the gas

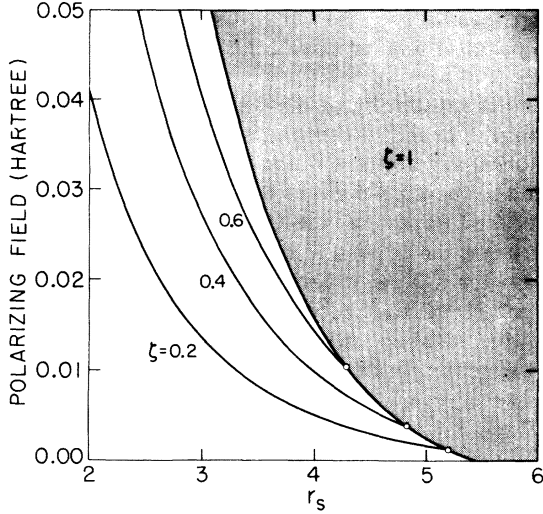


FIG. 1. Magnetic phase diagram for a HF gas. For each  $r_s < 5.45$  there is a critical field at which the relative magnetization jumps from some  $\zeta < 1$  to  $\zeta = 1$ . For  $r_s > 5.45$  the HF gas is fully magnetized even in the absence of a polarizing field. A polarizing field of 0.01 Hartree or 0.27 eV corresponds to a magnetic field of 47 million G.

is paramagnetic while for large  $r_s$  and  $\epsilon_x \gg \epsilon_k$  the gas becomes ferromagnetic.

### B. Random-phase approximation

At metallic electron densities, where the interaction energy and kinetic energy of an electron gas are comparable, one anticipates that the Coulomb repulsion between electrons will play an important role in electron correlation. Since the Coulomb interaction does not depend on spin, both spin-parallel and spin-antiparallel pairs of electrons are correlated by the Coulomb force. When Coulomb derived correlation is taken into account, the difference in interaction energy of electron pairs with parallel and antiparallel spins is reduced from what it was in the HF approximation. This fact suggests that higher-order approximations such as the RPA will yield a paramagnetic ground state at much lower densities than the HF.

The RPA has been applied to an electron gas assumed to be polarized in the absence of a polarizing field by von Barth and Hedin<sup>5</sup> and by Lam<sup>16</sup> who obtain the correlation energy as a function of  $r_s$  and  $\zeta$ . When the RPA is applied to the electron gas in the presence of a polarizing field,<sup>17</sup> it is found that the correlation energy is unchanged. Thus, the energy per particle of the spin-polarized gas in the RPA can be written

$$\epsilon_{\text{RPA}} = \epsilon_m + \epsilon_k + \epsilon_x + \epsilon_{\text{C,RPA}}, \quad (2.7)$$

where  $\epsilon_{\text{C,RPA}}$  is the correlation energy calculated by

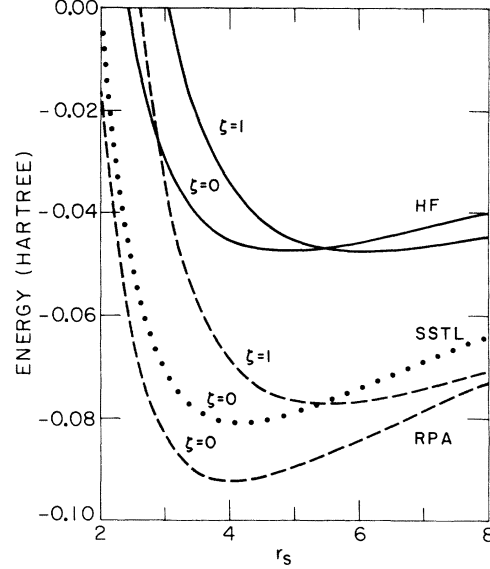


FIG. 2. Energy per particle of an electron gas in the absence of a polarizing field for relative magnetizations of 0 and 1. Results are shown for the HF, RPA, and SSTL approximations.

von Barth and Hedin and Lam. In the present work we adopt the parametrization for  $\epsilon_{\text{C,RPA}}(r_s, \zeta)$  suggested by von Barth and Hedin, namely,

$$\epsilon_{\text{C,RPA}} = \epsilon_c^P(r_s) \frac{2^{4/3} - (1+\zeta)^{4/3} - (1-\zeta)^{4/3}}{2(2^{1/3} - 1)} + \epsilon_c^F(r_s) \frac{(1+\zeta)^{4/3} + (1-\zeta)^{4/3} - 2}{2(2^{1/3} - 1)}, \quad (2.8)$$

where  $\epsilon_c^P$  and  $\epsilon_c^F$  are the correlation energies of the paramagnetic ( $\zeta = 0$ ) and ferromagnetic ( $\zeta = 1$ ) states for which the following parametrizations are suggested:

$$\epsilon_c^P(r_s) = -C_P F(r_s/r_P), \quad (2.9)$$

$$\epsilon_c^F(r_s) = -C_F F(r_s/r_F), \quad (2.10)$$

$$F(Z) = (1+Z^3) \ln(1+1/Z) - Z^2 + \frac{1}{2}Z - \frac{1}{3}, \quad (2.11)$$

with  $C_P = 0.0252e^2/a_0$ ,  $C_F = 0.0127e^2/a_0$ ,  $r_P = 30$ , and  $r_F = 75$ .

In Fig. 2 we show the energy per particle of an electron gas as a function of  $r_s$  and  $\zeta$  in the absence of a polarizing field for both the HF and RPA approximations. The RPA gas remains paramagnetic over the entire range of metallic densities even though the HF gas becomes ferromagnetic at  $r_s = 5.45$ . Lam<sup>16</sup> has calculated  $\epsilon_{\text{C,RPA}}$  for  $r_s = 12$  and finds a paramagnetic ground state even at this density.

The ground-state magnetization in the presence of a polarizing field is determined by selecting  $\zeta$  to minimize  $\epsilon_{\text{RPA}}$ . The equation obtained by setting

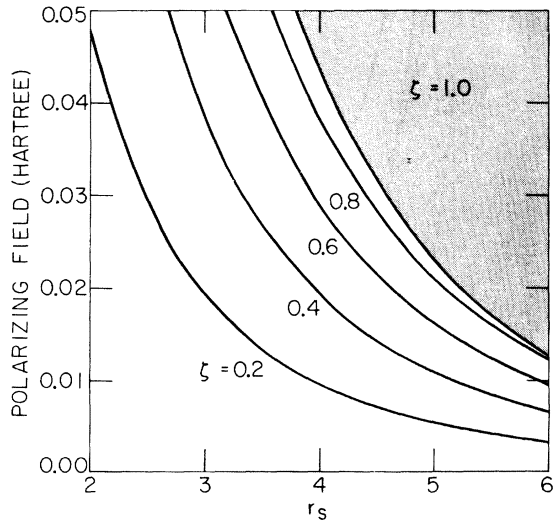


FIG. 3. Magnetic phase diagram of the RPA gas. As in the HF approximation, there is a critical field at which the relative magnetization jumps from some  $\zeta < 1$  to  $\zeta = 1$ .

$d\epsilon_{\text{RPA}}/d\zeta$  to zero determines most of the phase diagram shown in Fig. 3. As in the HF approximation, there is a critical field at which the relative magnetization jumps suddenly to one. At  $r_s = 6$  the jump occurs between  $\zeta = 0.84$  and  $\zeta = 1$ .

The accuracy of the RPA can be judged in part by comparing it with more accurate theories. In Fig. 2 we show the essentially exact results of Singwi *et al.*<sup>18</sup> (SSTL) for the total energy of the  $\zeta = 0$  gas. Although the RPA overestimates the correlation energy of the electron gas, the susceptibility calculated on the basis of the RPA energy functional by von Barth and Hedin<sup>5</sup> agrees with more accurate theories<sup>19</sup> to within a few percent.

### III. INHOMOGENEOUS SPIN-POLARIZED ELECTRON GAS

#### A. Density-functional formalism

Inhomogeneous systems present a difficult many-body problem simply because they lack translational symmetry. Because electron correlation often plays an essential role in inhomogeneous systems, it is important to find approximate methods for treating such many-body effects. The density-functional formalism is the basis of a number of such approximate methods.

In considering the density-functional formalism we restrict discussion to systems for which the inhomogeneities are determined by an external charge density  $\rho_e(\vec{r})$  and a polarizing field  $\vec{J}(\vec{r})$  with constant direction. If the direction of spin quantization is chosen to coincide with  $\vec{J}$ , then the electronic response of the system can be characterized

by  $n_+(\vec{r})$  and  $n_-(\vec{r})$ , the densities of electrons with spin parallel and antiparallel to the polarizing field.

The basic theorem of the density-functional formalism was proven first for the paramagnetic case by Hohenberg and Kohn<sup>3</sup> and has recently been extended to the spin-polarized case by von Barth and Hedin<sup>5</sup> and Rajagopal and Callaway.<sup>6</sup> The theorem states that the ground state energy of an electron gas is, for a given external charge density  $\rho_e(\vec{r})$  and polarizing field  $J(\vec{r})$ , a functional of the spin densities  $n_+(\vec{r})$  and  $n_-(\vec{r})$  and that this functional can be written in the form

$$E = \frac{1}{2} \int d^3r d^3r' \frac{[en(\vec{r}) + \rho_e(\vec{r})][en(\vec{r}') + \rho_e(\vec{r}')]}{|\vec{r} - \vec{r}'|} - \int d^3r [n_+(\vec{r}) - n_-(\vec{r})]J(\vec{r}) + G[n_+, n_-], \quad (3.1)$$

where  $G$  is a universal functional of the spin densities. The theorem further states that  $E$  is minimized by the correct spin densities.

The first term on the right-hand side of Eq. (3.1) is the electrostatic energy of the external and electronic charge densities; the second term is the magnetic energy associated with the polarizing field; and the third term includes the kinetic, exchange, and correlation energies of the electron gas. If the functional  $G$  is known, then we can use Eq. (3.1) to solve for the spin densities variationally based on the stationarity of  $E$ . Taking the variation of  $E$  with respect to the spin densities, subject the condition that the number of electrons  $N$  remain fixed, we obtain

$$\delta(E - \mu N)/\delta n_\sigma = 0, \quad (3.2)$$

where  $N = \int d^3r n(r)$ . The Lagrange multiplier  $\mu$  is the chemical potential.

While the density-functional formalism does not give an explicit form for  $G$ , it does state that  $G$  is a universal functional, the same for all electronic systems. In Secs. IIIB and IIIC, we derive approximate forms for  $G$  which allow correspondingly approximate solutions for the spin densities of inhomogeneous systems.

#### B. Gradient expansion

Following Hohenberg and Kohn who considered the paramagnetic case,<sup>3</sup> we define an energy-density functional  $g$  such that

$$G[n_+, n_-] = \int d^3r g[n_+, n_-] \quad (3.3)$$

and proceed by assuming that  $g$  can be expanded in terms of the gradients of  $n_+(\vec{r})$  and  $n_-(\vec{r})$ . Symmetry arguments based on the universality of  $G$  can be used to reduce such an expansion to one of

the form

$$g[n_+, n_-] = g_0(n_+, n_-) + g_2^+(n_+, n_-) |\vec{\nabla} n_+|^2 + g_2^-(n_+, n_-) |\vec{\nabla} n_-|^2 + g_2^{+-}(n_+, n_-) \vec{\nabla} n_+ \cdot \vec{\nabla} n_- + \dots \quad (3.4)$$

Here the coefficients  $g_0$  and  $g_2$  are functions and not functionals of  $n_+$  and  $n_-$ . An expansion of this form is valid only if the spin densities vary slowly with position.

In the uniform limit,  $g$  is equal to  $g_0$  and is simply the kinetic, exchange, and correlation energy per unit volume of the uniform electron gas. In terms of the energies per particle we have

$$g_0 = n(\epsilon_k + \epsilon_x + \epsilon_c), \quad (3.5)$$

where  $\epsilon_k$ ,  $\epsilon_x$ , and  $\epsilon_c$  are given by Eqs. (2.3), (2.4), and (2.8) written as functions of  $n_+$  and  $n_-$  rather than  $r_s$  and  $\zeta$ . The coefficients  $g_2$  of the second-order gradient terms are determined by linear-response theory. Using the RPA linear response functions we obtain<sup>17</sup>

$$g_2^\sigma = \frac{1}{\hbar^2} (\hbar^2/m) 1/n_\sigma, \quad g_2^{+-} = 0. \quad (3.6)$$

These coefficients, accurate in the limit of high densities, account only for kinetic contributions to the gradient term. Exchange and correlation corrections to  $g_2$  are obtained in theories that go beyond the RPA. These terms are difficult to evaluate and are just beginning to be understood in the paramagnetic limit.<sup>20</sup>

Physically, the gradient expansion may be interpreted as follows. In approximating  $g$  by  $g_0$  one assumes that at each point of the inhomogeneous system the local momentum distribution and correlation hole are the same as those of a uniform electron gas with a density equal to the local density. The kinetic part of the gradient expansion accounts for the fact that high-momentum components are required to construct a rapidly changing electron density. The exchange and correlation gradient term accounts for distortions of the correlation hole which result from nonuniformities in the density.

### C. Method of Kohn and Sham

Hohenberg and Kohn<sup>3</sup> have pointed out that the gradient expansion does not properly account for the discontinuity in occupation number at the Fermi surface and consequently fails to reproduce the  $q = 2k_F$  Friedel oscillations in the electron density. The method of Kohn and Sham<sup>4</sup> overcomes this problem by breaking  $G$  into a kinetic and an exchange-correlation part

$$G[n_+, n_-] = T[n_+, n_-] + E_{xc}[n_+, n_-] \quad (3.7)$$

and treating the kinetic part exactly.  $T$  is defined to be the kinetic energy of a noninteracting electron gas with spin densities  $n_+$  and  $n_-$  and  $E_{xc}$  is defined by Eq. (3.7).

The basic theorem of the Kohn and Sham method was originally proven for the paramagnetic gas but it can easily be extended to the spin-polarized case.<sup>5,6</sup> The theorem states that the spin densities of an interacting electron gas, defined by a given external charge distribution and polarizing field, are equal to the spin densities of a noninteracting gas in the presence of an effective potential. That is, if we solve the single-particle Schrödinger equation

$$[-(\hbar^2/2m)\nabla^2 + V_{\text{eff}}^\sigma(\vec{r})] \psi_{i\sigma}(\vec{r}) = \hbar\omega_{i\sigma} \psi_{i\sigma}(\vec{r}), \quad (3.8)$$

and compute the spin densities assuming the states of lowest energy are occupied,

$$n_\sigma(\vec{r}) = \sum_i |\psi_{i\sigma}(\vec{r})|^2, \quad (3.9)$$

then these will equal the spin densities of the interacting problem, provided  $V_{\text{eff}}^\sigma$  is given by

$$V_{\text{eff}}^\sigma(\vec{r}) = e\varphi(\vec{r}) - \sigma J(\vec{r}) + \delta E_{xc}/\delta n_\sigma, \quad (3.10)$$

where  $\varphi$  is the electrostatic potential. Since  $V_{\text{eff}}^\sigma$  depends on the spin densities themselves, we must solve Eqs. (3.8)–(3.10) self-consistently. The kinetic energy may be computed as the difference between the total energy and the potential energy of the noninteracting system

$$T = \sum_{i\sigma} \hbar\omega_{i\sigma} - \sum_\sigma \int d^3r V_{\text{eff}}^\sigma n_\sigma. \quad (3.11)$$

The method of Kohn and Sham becomes approximate when we use an approximate form for the exchange and correlation part of the effective potential  $\delta E_{xc}/\delta n_\sigma$ . Such approximate forms can be obtained directly from the gradient expansion by omitting the kinetic part of  $G$ . If gradient terms are neglected we obtain the local density approximation for the effective potential

$$V_{\text{eff}}^\sigma = e\varphi - \sigma J + \mu_{xc}^\sigma, \quad (3.12)$$

where

$$\mu_{xc}^\sigma = \frac{\partial}{\partial n_\sigma} [n(\epsilon_x + \epsilon_c)]. \quad (3.13)$$

A number of approximations for the local exchange-correlation potential  $\mu_{xc}^\sigma$  can be obtained depending on how we evaluate  $\epsilon_c$ , the correlation energy per particle of the uniform gas. We will consider three approximations, namely, those which result from the HF, RPA, and SSTL approximations for  $\epsilon_c$ . In the HF approximation,  $\epsilon_c$  is zero and the effective exchange and correlation potential becomes

$$\mu_{xc, HF}^{\sigma} = -e^2 (6/\pi)^{1/3} n^{1/3}. \quad (3.14)$$

This result was first derived in the above fashion by Kohn and Sham<sup>4</sup> and is now commonly used in band calculations. The RPA result for  $\mu_{xc}^{\sigma}$  is much more complicated than  $\mu_{xc, HF}^{\sigma}$  but can be derived directly from Eqs. (2.8) and (3.13).<sup>5</sup> It should be noted that the extra complication of using  $\mu_{xc, RPA}^{\sigma}$  instead of  $\mu_{xc, HF}^{\sigma}$  is insignificant in terms of the computer time required for a self-consistent calculation. More important differences between the HF and RPA effective exchange and correlation potentials are shown in Fig. 4 where the potentials are plotted as a function of relative magnetization for a given density. The RPA potential is more negative than the HF potential, reflecting the energy lowering due to Coulomb-derived correlations in the RPA. One also notes that the potential for minority-spin electrons goes to zero in the limit of low minority-spin densities for the HF but not for the RPA. This is accounted for by the fact that spin-antiparallel electrons are correlated in the RPA but not in the HF.

We also consider an essentially exact local effective potential for the paramagnetic case based the SSTL approximation of Singwi *et al.*<sup>18</sup> Hedin

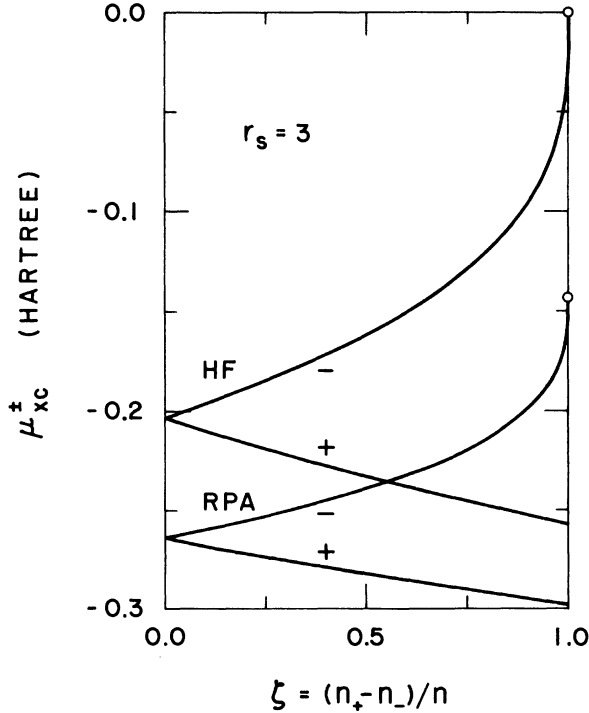


FIG. 4. Effective exchange and correlation potential in the HF and RPA as a function of relative magnetization for  $r_s = 3$ . The curves labeled + and - are the potentials for majority- and minority-spin electrons, respectively. Circles indicate the end points of the minority-spin potentials at  $\zeta = 1$ .

and Lundquist<sup>21</sup> have shown that  $\epsilon_{c, SSTL}$  is accurately reproduced by the function  $\epsilon_c^P(r_s)$  [Eq. (2.8)], with  $C_p = 0.0225 e^2/a_0$  and  $r_p = 21$  and they derive the corresponding  $\mu_{xc, SSTL}$ . This potential is used to check the accuracy of our results, obtained using the HF and RPA potentials, in the paramagnetic limit.

#### IV. EQUATIONS FOR THE SPIN-POLARIZED SURFACE

In this section we specialize the results of Secs. II and III to the surface of a spin-polarized gas. Two model systems are considered. The first system, which applies to a simple metal in a uniform magnetic field, is defined by the following external charge density and polarizing field:

$$\rho_e(\vec{r}) = -en_0\Theta(-x), \quad (4.1)$$

$$J(\vec{r}) = J_0. \quad (4.2)$$

Here  $n_0$  is the electron density in the bulk and  $\rho_e$  represents a neutralizing charge density which ends abruptly at the  $x = 0$  plane. The polarizing field  $J_0$  represents a magnetic field  $B = J_0/\mu_B$ . The second model system applies to ferromagnetic gadolinium and is defined by the same external charge density as the first model but assumes a polarizing field of the form

$$J(\vec{r}) = J_0\Theta(-x), \quad (4.3)$$

which simulates the disappearance of the  $4f$  exchange field at the surface. The properties of both models are a function of just two parameters  $n_0$  and  $J_0$ . Both models also possess sufficient symmetry that the resulting spin densities and effective potentials depend only on  $x$ , a fact which greatly simplifies the surface equations.

In obtaining solutions for these two models we consider two different methods, a highly approximate parametrized-variational method and an accurate self-consistent method. Before considering the details of these methods we discuss the charge neutrality condition, the surface magnetization, the work function, and the surface energy.

##### A. Surface properties

The charge-neutrality condition results if we require that the electric field be zero both in the metal's interior and in the vacuum. Applying this restriction, we obtain the sum rule

$$\int_{-\infty}^{\infty} dx [n(x) - n_0\Theta(-x)] = 0, \quad (4.4)$$

which simply requires that the total charge of the system be zero. (In a field emission experiment the electric field is nonzero in the vacuum region and a net charge is associated with the surface.)

While the electronic charge density  $e(n_+ + n_-)$  satisfies a definite sum rule at the surface, there is no corresponding sum rule for the magnetization  $\mu_B(n_+ - n_-)$ . This leads us to define a quantity  $M_s$  called the surface magnetization:

$$M_s = \mu_B \int_{-\infty}^{\infty} dx [n_+(x) - n_-(x) - (n_{0+} - n_{0-})\Theta(-x)]. \quad (4.5)$$

Here  $n_{0+}$  and  $n_{0-}$  are the bulk spin densities.  $M_s$  is the excess magnetization associated with the surface or, more precisely, the change in total moment which results when a solid is cleaved divided by the surface area formed by cleavage.

The work function  $\Phi$  is defined as the minimum energy required to remove an electron from a solid into the vacuum. Lang and Kohn<sup>2</sup> have shown that the work function is obtained rigorously from a naive interpretation of the effective-potential picture. That is, the work function is simply the difference in the effective single-particle energies of an electron at rest in the vacuum and an electron at the Fermi level in the bulk:

$$\Phi = V_{\text{eff}}^{\sigma}(\infty) - [V_{\text{eff}}^{\sigma}(-\infty) + \hbar^2 k_F^2 / 2m]. \quad (4.6)$$

In cases where  $J$  is nonzero in the vacuum, Eq. (4.6) yields a different work function for spin + and - electrons, as is physically correct. In order to obtain a single value for the work function, we shall assume that the polarizing field goes to zero far from the surface. In this case, the work function is given by

$$\Phi = e[\varphi(\infty) - \varphi(-\infty)] + \sigma J_0 - \mu_{xc}^{\sigma}(n_{0+}, n_{0-}) - \hbar^2 k_F^2 / 2m. \quad (4.7)$$

The surface energy of a solid is the energy required to cleave the solid per unit area of surface formed. For the spin-polarized gas, it is useful to break the total surface energy  $\sigma$  into electrostatic, magnetic, kinetic, exchange, and correlation parts

$$\sigma = \sigma_e + \sigma_m + \sigma_k + \sigma_x + \sigma_c. \quad (4.8)$$

Using the gradient expansion developed in Sec. III, we can express the surface energy in terms of the spin densities

$$\sigma_e = \frac{e}{2} \int_{-\infty}^{\infty} dx [\varphi(x) - \varphi(-\infty)] [n(x) - n_0 \Theta(-x)], \quad (4.9)$$

$$\sigma_m = - \sum_{\sigma} \int_{-\infty}^{\infty} dx \sigma J(x) [n_{\sigma}(x) - n_{0\sigma} \Theta(-x)], \quad (4.10)$$

$$\sigma_k = \frac{3^{5/3} \pi^{4/3}}{2^{1/35}} \frac{\hbar^2}{m} \sum_{\sigma} \int_{-\infty}^{\infty} dx [n_{\sigma}^{5/3}(x) - n_{0\sigma}^{5/3} \Theta(-x)] + \frac{1}{72} \frac{\hbar^2}{m} \sum_{\sigma} \int_{-\infty}^{\infty} dx \frac{1}{n_{\sigma}(x)} \left( \frac{dn_{\sigma}}{dx} \right)^2, \quad (4.11)$$

$$\sigma_x = - \frac{3^{4/3}}{2^{5/3} \pi^{1/3}} e^2 \sum_{\sigma} \int_{-\infty}^{\infty} dx [n_{\sigma}^{4/3}(x) - n_{0\sigma}^{4/3} \Theta(-x)], \quad (4.12)$$

$$\sigma_c = \int_{-\infty}^{\infty} dx [n(x) \epsilon_c(n_+(x), n_-(x)) - n_0 \epsilon_c(n_{0+}, n_{0-}) \Theta(-x)], \quad (4.13)$$

where the electrostatic potential  $\varphi$  is given by

$$\varphi(x) = -4\pi e \int_{-\infty}^x dx' \int_{-\infty}^{x'} dx'' [n(x'') - n_0 \Theta(-x'')]. \quad (4.14)$$

### B. Parametrized variational solution

A variational solution for the spin densities at a surface can be obtained by direct minimization of the surface energy with respect to the spin densities. Using the calculus of variations, we can derive a set of differential equations for the spin densities from the gradient expansion of the surface-energy functional. Warner<sup>22</sup> has carried out a numerical solution of these equations for the paramagnetic case and obtains work functions comparable to those of Lang and Kohn.<sup>2</sup> Smith<sup>23</sup> introduced a less-rigorous but easily executed method, which was recently applied to a spin-polarized surface by Pant and Rajagopal.<sup>24</sup> In this method one assumes that the spin densities are of a simple parametrized form and then solves for the spin densities by adjusting the parameters to minimize the surface energy. We adopt the following form for the spin densities:

$$n_{\sigma}(x) = \begin{cases} n_{0\sigma} (1 - \frac{1}{2} e^{B_{\sigma}(x-x_{\sigma})}), & x < x_{\sigma}, \\ n_{0\sigma}^{\frac{1}{2}} e^{-B_{\sigma}(x-x_{\sigma})}, & x > x_{\sigma}. \end{cases} \quad (4.15)$$

This parametrized form was chosen to asymptotically approach the bulk spin densities in the interior and zero density in the vacuum. It is defined by the four parameters  $B_+$ ,  $B_-$ ,  $x_+$ , and  $x_-$ . However, the charge neutrality condition imposes the restriction that  $x_+ n_{0+} + x_- n_{0-} = 0$ ; reducing the number of adjustable parameters to three. Pant and Rajagopal adopt a similar form for the spin densities but assume that  $B_+ = B_-$  and  $x_+ = x_- = 0$  and thereby exclude the possibility of a net surface magnetization.

With the exception of the correlation term, the integrals involved in computing the surface energy

can be evaluated in closed form for the spin densities given by Eq. (4.15).<sup>17</sup> Thus, if the correlation energy is neglected, the surface energy can be written as an explicit function of  $B_+$ ,  $B_-$ , and  $x_+$ . By adjusting these three parameters to minimize the surface energy, we obtain an approximate solution for a spin-polarized surface. This method is applied to the Gd model in Sec. V.

### C. Self-consistent solution

In the method of Kohn and Sham we obtain the spin densities for a system of interacting electrons in the presence of an external charge density and polarizing field by solving for the spin densities of a system of noninteracting electrons in the presence of an effective potential. We first apply this method to the bulk spin-polarized gas. In the bulk, the effective potential is a constant for each spin

$$V_{\text{eff}}^\sigma(-\infty) = e\varphi(-\infty) - \sigma J_0 + \mu_{xc}^\sigma(n_{0+}, n_{0-}) \quad (4.16)$$

and the solutions of the resulting Schrödinger equation are plane waves with energies given by

$$\hbar\omega_{\vec{k}\sigma}^\sigma = V_{\text{eff}}^\sigma(-\infty) + \hbar^2 k^2 / 2m. \quad (4.17)$$

Given  $V_{\text{eff}}^\sigma(-\infty)$ , the ground state can be constructed by filling the plane-wave states in order of increasing energy until the total density of electrons is  $n_0$ . This determines the bulk spin densities

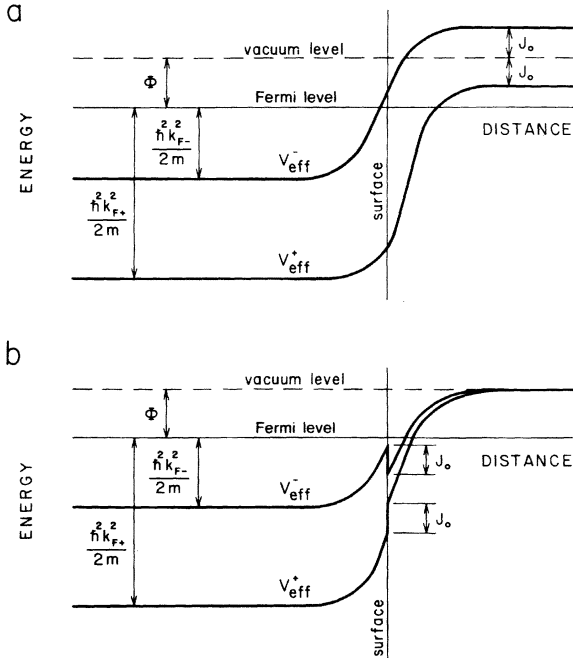


FIG. 5. Spin-dependent effective potentials (a) for the surface model  $J(\vec{r}) = J_0$  and (b) for the surface model  $J(\vec{r}) = J_0 \theta(-x)$ .

$n_{0+}$  and  $n_{0-}$ . However, because  $V_{\text{eff}}^\sigma(-\infty)$  is itself dependent on  $n_{0+}$  and  $n_{0-}$ , the problem must be solved self-consistently to obtain the correct spin densities. If  $\mu_{xc}^\sigma$  is approximated by  $\mu_{xc, \text{HF}}^\sigma$  then this procedure obtains the same result for the bulk magnetization as obtained in Sec. II from the HF approximation (except where  $\zeta$  jumps suddenly to 1). Similarly, using  $\mu_{xc, \text{RPA}}$  leads to the RPA result of Sec. II. Thus, the method of Kohn and Sham reproduces that solution of the uniform gas from which the effective exchange and correlation potential was derived.

Spin-dependent effective potentials for the two surface models are sketched in Fig. 5. In the bulk, the Fermi level lies at an energy  $\hbar^2 k_{F+}^2 / 2m$  above  $V_{\text{eff}}^\sigma(-\infty)$  and  $\hbar^2 k_{F-}^2 / 2m$  above  $V_{\text{eff}}^\sigma(-\infty)$ . The effective spin splitting of the conduction band  $V_{\text{eff}}^- - V_{\text{eff}}^+$  is  $2J_0 + \mu_{xc}^-(n_{0+}, n_{0-}) - \mu_{xc}^+(n_{0+}, n_{0-})$  in the bulk for both models. For the model corresponding to a simple metal in a magnetic field the effective splitting in the vacuum is  $2J_0$  or just that due to the magnetic field. For the gadolinium model the splitting is zero in the vacuum since the polarizing field drops to zero at the surface.

To calculate the spin densities at the surface for a given effective potential, we must solve the single-particle Schrödinger equation

$$\left( -\frac{\hbar^2}{2m} \nabla^2 + V_{\text{eff}}^\sigma(x) \right) \psi_{\vec{k}\sigma}^\sigma(\vec{r}) = \hbar\omega_{\vec{k}\sigma}^\sigma \psi_{\vec{k}\sigma}^\sigma(\vec{r}). \quad (4.18)$$

Because the solutions of this equation are plane waves in the bulk, it is convenient to label the eigenstates by their bulk momentum  $\vec{k}$ . The single-particle energies are given by Eq. (4.17). To take advantage of the one-dimensional structure of the problem we write

$$\psi_{\vec{k}\sigma}^\sigma(\vec{r}) = \psi_{k_x\sigma}(x) e^{i(k_y y + k_z z)} \quad (4.19)$$

and require that  $\psi_{k_x\sigma}$  approach a sine wave of unit amplitude in the interior:

$$\psi_{k_x\sigma}(x) \xrightarrow{x \rightarrow -\infty} \sin[k_x x - \gamma_\sigma(k_x)]. \quad (4.20)$$

The asymptotic phase  $\gamma_\sigma(k_x)$  is defined unambiguously by taking  $\gamma_\sigma(0) = 0$  and requiring that  $\gamma_\sigma$  be a continuous function of  $k_x$ . The one-dimensional Schrödinger equation for  $\psi_{k_x\sigma}$  which results from Eqs. (4.18) and (4.19) is

$$\left( -\frac{\hbar^2}{2m} \frac{d^2}{dx^2} + V_{\text{eff}}^\sigma(x) - V_{\text{eff}}^\sigma(-\infty) \right) \psi_{k_x\sigma}(x) = \frac{\hbar^2 k_x^2}{2m} \psi_{k_x\sigma}(x). \quad (4.21)$$

After solving Eq. (4.21) for values of  $k_x$  between 0 and  $k_{F\sigma}$ , we calculate the spin density using the formula

$$n_\sigma(x) = \frac{1}{2\pi^2} \int_0^{k_{F\sigma}} dk_x (k_{F\sigma}^2 - k_x^2) |\psi_{k_x\sigma}(x)|^2. \quad (4.22)$$



Equation (4.21) and (4.22) allow us to compute the spin densities for a given effective potential. Equation (3.12) relates the effective potential to the spin densities. The surface problem is solved when the spin densities which result from solving the Schrödinger equation are the same as those which determine the effective potential and simultaneously satisfy the charge neutrality condition, Eq. (4.4). The method used to obtain self-consistency is discussed in the Appendix.

By definition, the kinetic term of the energy functional is the kinetic energy of a noninteracting gas with the same densities as the interacting gas. In the method of Kohn and Sham the kinetic term is easily computed by taking the difference between the total energy and the effective potential energy of the noninteracting system. The resulting kinetic surface energy is

$$\sigma_k = \frac{1}{4\pi^2} \frac{\hbar^2}{m} \sum_{\sigma} \int_0^{k_{F\sigma}} dk_x k_x (k_{F\sigma}^2 - k_x^2) \left[ \frac{1}{4}\pi - \gamma_{\sigma}(k_x) \right] - \sum_{\sigma} \int_{-\infty}^{\infty} dx n_{\sigma}(x) [V_{\text{eff}}^{\sigma}(x) - V_{\text{eff}}^{\sigma}(-\infty)]. \quad (4.23)$$

The first term on the right-hand side of this equation is the total surface energy of the noninteracting system as derived by Huntington.<sup>25</sup> The total surface energy in the method of Lang and Kohn is obtained from the gradient expansion Equation (4.9)–(4.13) with the kinetic term replaced by Eq. (4.23).

#### D. Sum rules

Two sum rules check the accuracy of the self-consistent solutions presented in the next section. The sum rules for the spin-polarized case represent simple extensions of existing paramagnetic sum rules and are stated here without proof.

A sum rule for the asymptotic phase  $\gamma$  was first demonstrated by Sugiyama.<sup>26</sup> The rule states that a weighted average of the asymptotic phase equals  $\frac{1}{4}\pi$ . In the spin-polarized case, this becomes

$$\frac{2}{k_{F+}^2 + k_{F-}^2} \sum_{\sigma} \int_0^{k_{F\sigma}} dk_x k_x \gamma_{\sigma}(k_x) = \frac{1}{4}\pi. \quad (4.24)$$

This sum rule is derived directly from the charge neutrality condition and is quite generally valid.<sup>27</sup>

A sum rule on the difference in electrostatic potential between the bulk and the surface plane has been derived by Vannimenus and Budd<sup>28</sup> for a surface with the external charge density given in Eq. (4.1). In the presence of a polarizing field this rule is

$$e[\varphi(0) - \varphi(-\infty)] - \frac{n_+(0) - n_-(0)}{n_0} \times [J(0+) - J(0-)] = n_0 \frac{\partial \epsilon}{\partial n_0}, \quad (4.25)$$

where  $\epsilon$  is the energy per particle of the uniform gas. This sum rule, based on the density-functional formalism, will be satisfied by any calculation which accurately minimizes the total energy, provided  $\epsilon$  is chosen to correspond with the assumed energy functional. Note that the second term on the left-hand side of Eq. (4.25) is non-zero only when there is a discontinuity in the polarizing field at the surface.

For the self-consistent calculations presented here, the above sum rules were generally satisfied to within 0.2%. Our calculation was also checked by repeating the calculation of Lang and Kohn<sup>1</sup> using their interpolation formula for  $\epsilon_c$ . Agreement was better than one percent for all calculated quantities for a bulk density of  $r_s = 3$ .

## V. RESULTS

### A. Paramagnetic limit

In the  $J_0 = 0$  limit, both of the spin-polarized surface models we consider reduce to the paramagnetic model of Lang and Kohn.<sup>1</sup> We have repeated the self-consistent calculation of Lang and Kohn using the RPA effective exchange and correlation

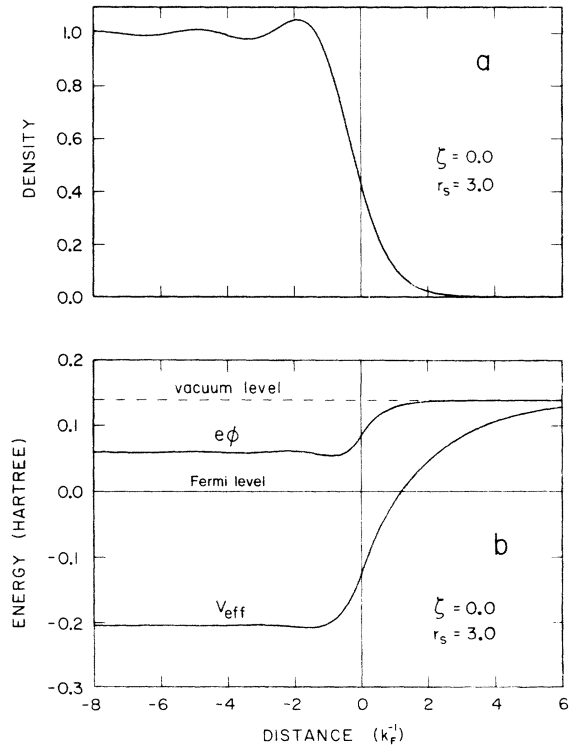


FIG. 6. Electron density, electrostatic potential, and effective potential at the surface of a paramagnetic electron gas for  $r_s = 3$ . Results are for a self-consistent calculation using the RPA energy functional. The distance scale is in units of  $1/k_F = 0.0827$  nm.

potential. In obtaining this solution we purposely chose trial spin densities with a net surface magnetization. The self-consistent solutions nevertheless obtained spin + and - densities which were identical to within calculational accuracy. This confirms the implicit assumption of Lang and Kohn that the surface of a paramagnetic gas is also paramagnetic.

The electron density, electrostatic potential, and effective potential which result for the surface of a paramagnetic gas of density  $r_s = 3$  are shown in Fig. 6. The oscillations in electron density are the anticipated Friedel oscillations of wave number  $2k_F$ .

### B. Susceptibility of the paramagnetic surface

The system defined by Eqs. (4.1) and (4.2) models the surface of a simple metal in a uniform magnetic field. Using the RPA exchange and correlation potential, we have obtained for this model the self-consistent spin densities for several values of electron density and magnetic field. When the magnetic field  $B = J_0/\mu_B$  is sufficiently small, we find that the magnetization  $M(x) = \mu_B[n_+(x) - n_-(x)]$  is proportional to the field. Thus, we define a position-dependent susceptibility

$$\chi(x) = \lim_{B \rightarrow 0} \frac{M(x)}{B}, \quad (5.1)$$

which specifies the magnetic response of the gas to a uniform magnetic field.

In the bulk,  $\chi(x)$  reduces to the susceptibility of the uniform electron gas  $\chi_0$ . The values of  $\chi_0$  calculated using the RPA energy functional, originally obtained by von Barth and Hedin,<sup>5</sup> are listed in Table I. The average measured susceptibility of sodium ( $r_s = 3.99$ ) is<sup>29</sup>  $115 \times 10^{-9} \mu_B/\text{nm}^3 \text{G}$  in good agreement with our value for  $r_s = 4$ . The position-dependent susceptibility  $\chi(x)$  was calculated by solving for the magnetization resulting from a weak magnetic field. Our results for several values of bulk electron density are shown in Fig. 7. The oscillations in the magnetization are of wave number  $2k_F$ .

While it would be difficult to measure the de-

TABLE I. Bulk susceptibility  $\chi_0$  and surface susceptibility  $\chi_s$  as a function of  $r_s$  obtained using the RPA energy functional.  $\chi_0$  is in units of  $10^{-9} \mu_B/\text{nm}^3 \text{G}$  and  $\chi_s$  is in units of  $10^{-9} \mu_B/\text{nm}^2 \text{G}$ .

$r_s$	2	3	4	5
$\chi_0$	179	133	112	101
$\chi_s$	10.4	7.9	6.4	5.8

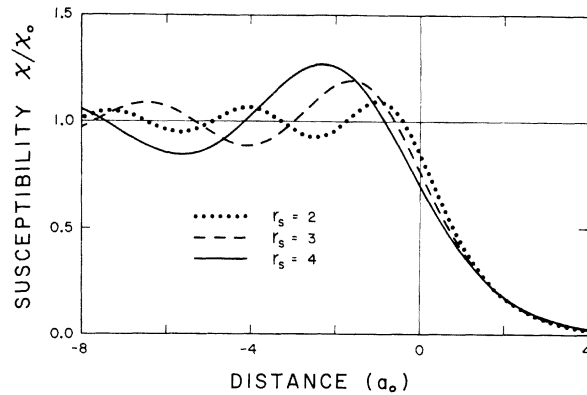


FIG. 7. Position-dependent susceptibility at the surface of an electron gas for several values of  $r_s$ . The distance scale is in units of  $a_0 = 0.0529 \text{ nm}$ .

tailed spatial dependence of the magnetization shown in Fig. 7, it might be possible to measure an average magnetic surface response. The average surface response is characterized by the surface susceptibility  $\chi_s$  defined by

$$\chi_s = \lim_{B \rightarrow 0} \frac{M_s}{B}, \quad (5.2)$$

where  $M_s$  is the surface magnetization [Eq. (4.5)]. Values of  $\chi_s$  are listed in Table I for several values of  $r_s$ . To get a feeling for the magnitude of the surface susceptibility, we consider the (110) surface of sodium. If we associate the induced surface magnetization entirely with atoms of the first surface layer then the surface susceptibility is  $8.05 \times 10^{-10} \mu_B/\text{G}$  per atom, assuming  $r_s = 4$ . This is to be compared with a bulk susceptibility of  $4.22 \times 10^{-9} \mu_B/\text{G}$  per atom. Thus, the surface susceptibility corresponds to a 19% increase in susceptibility for atoms of the surface layer of sodium. For lithium and potassium the corresponding figures are 24% and 15%.

### C. Surface of a model itinerate ferromagnet

The system defined by Eqs. (4.1) and (4.3) represents a simple model for an itinerant ferromagnet which derives from ferromagnetic gadolinium. Solutions for this model have been obtained using three different methods: (i) the parametrized-variational (PV) method discussed in Sec. IV B using the HF energy functional, (ii) the self-consistent (SC) method discussed in Sec. IV C using the HF energy functional, and (iii) the SC method using the RPA energy functional. Each of these methods was used to calculate the surface properties of an electron gas of density  $r_s = 3$  as a function of the bulk magnetiza-

tion  $\zeta$ . The major results are presented in Table II.

The PV method represents a simple but approximate approach to the surface problem. The accuracy of the PV method is largely dependent on the parametrized form assumed for the spin densities. Although the variational freedom of the parametrized form we have chosen [Eq. (4.15)] is quite limited, there is general agreement between the PV solution and the more accurate SC solution. Comparing the PV and SC solutions based on the HF energy functional (Tables IIA and IIB), one notes agreement, number for number, in the paramagnetic case and similar trends as the magnetization increases from  $\zeta = 0.0$  to 0.8.

Differences between these two solutions result both from the limited variational freedom of the PV solution and the different kinetic energy functionals of PV and SC methods. If complete variational freedom were allowed, the PV solution would satisfy the potential sum rule exactly. The sum-rule potential obtained by the present PV solution is too large by a factor of about 1.3. This suggests that a less-restrictive parametrization would improve the accuracy. However, the approximate nature of the PV kinetic energy func-

tional precludes the possibility of obtaining the Friedel oscillations of the SC solution.

The SC solutions presented in Tables IIB and IIC are both numerically accurate. They differ only in that they assume respectively the HF and RPA approximations for the local exchange and correlation potential. A comparison of these two potentials is of some interest because the HF potential, while commonly used in band calculations, is in principle less accurate than the RPA potential. In the paramagnetic limit the HF and RPA results are in substantial agreement but the HF solution underestimates both the surface energy and the work function. These underestimates are a direct reflection of the fact that the HF approximation neglects Coulomb derived correlations. With increasing bulk magnetization, the trends in most quantities are similar for the HF and RPA solutions but there is a general decline in agreement on a number for number basis. One notes in particular the discrepancies in the surface magnetization and surface energy at large polarizations. The fact that the HF solution overestimates  $M_s$  by a factor of about 4 is explained by the fact that the HF approximation neglects correlation between electrons of parallel spin and

TABLE II. Polarizing field  $J_0$ , work function  $\Phi$ , electrostatic dipole potential  $e\Delta\varphi = e[\varphi(\infty) - \varphi(-\infty)]$ , surface magnetization  $M_s$ , and surface energies as a function of  $\zeta$  for the model  $J(\vec{r}) = J_0\Theta(-x)$  with  $r_s = 3.0$ .  $J_0$ ,  $\Phi$ , and  $e\Delta\varphi$  are in eV;  $M_s$  is in  $\mu_B/\text{nm}^2$ ; and surface energies are in  $\text{erg}/\text{cm}^2$ . Results are given for several methods of solution in order of decreasing approximation.

$\zeta$	$J_0$	$\Phi$	$e\Delta\varphi$	$M_s$	$\sigma$	$\sigma_e$	$\sigma_m$	$\sigma_k$	$\sigma_x$	$\sigma_c$
A. Parametrized variational method—HF energy functional										
0.0	0.0	2.24	2.27	0.0	57	124	0	-685	617	0
0.2	0.37	2.23	2.26	0.09	60	124	12	-691	616	0
0.4	0.74	2.20	2.23	0.21	68	121	45	-706	609	0
0.6	1.10	2.15	2.19	0.41	79	118	93	-716	585	0
0.8	1.42	2.10	2.17	0.63	85	120	148	-718	535	0
B. Self-consistent method—HF energy functional										
0.0	0.0	2.54	2.56	0.0	127	190	0	-772	709	0
0.2	0.37	2.51	2.53	0.27	96	187	6	-794	697	0
0.4	0.74	2.45	2.48	0.64	-20	182	13	-864	648	0
0.6	1.10	2.39	2.43	1.16	-285	175	-1	-990	531	0
0.8	1.42	2.34	2.42	1.96	-855	172	-104	-1150	226	0
C. Self-consistent method—RPA energy functional										
0.0	0.0	3.77	2.15	0.0	247	159	0	-691	662	117
0.2	0.52	3.76	2.13	0.066	247	156	16	-701	659	117
0.4	1.04	3.72	2.06	0.17	238	148	61	-734	645	118
0.6	1.57	3.67	1.94	0.33	198	134	123	-794	611	124
0.8	2.11	3.60	1.79	0.41	160	117	232	-894	576	129
D. Self-consistent method—SSTL energy functional										
0.0	0.0	3.45	2.21	0.0	228	163	0	-702	668	99

thus overestimates the reduction in potential energy gained by polarization. One concludes that the HF exchange and correlation potential can lead to substantial errors in the spin-polarized surface problem, particularly in the limit of large polarizations.

Because the RPA is known to overestimate the correlation energy of an electron gas, we have repeated the paramagnetic surface calculation using the essentially exact SSTL local exchange and correlation potential. The results, given in Table

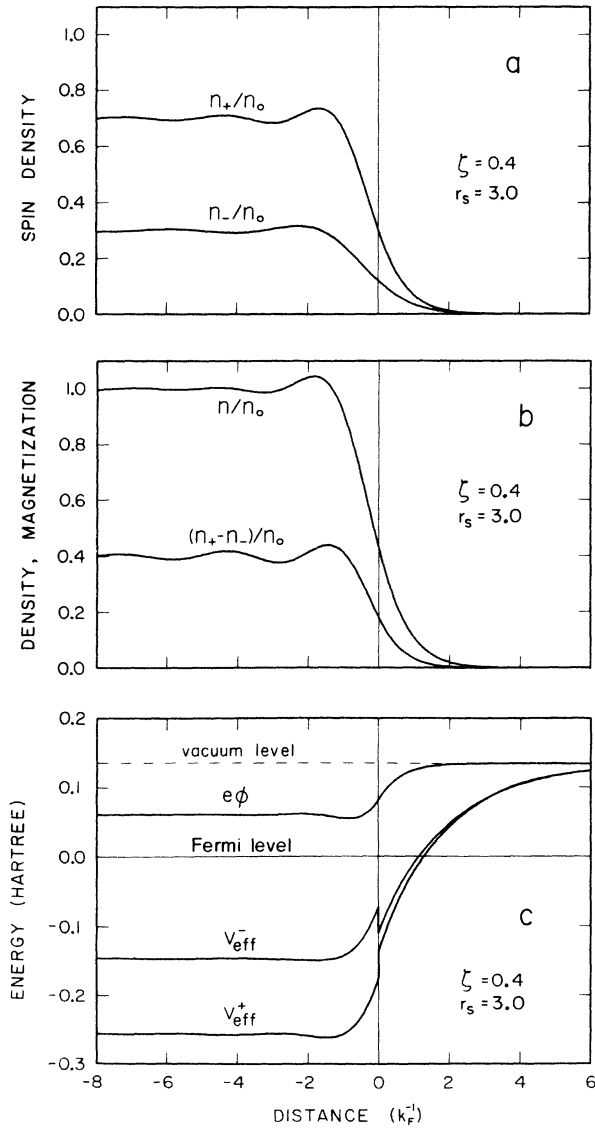


FIG. 8. Spin densities, total density, magnetization, electrostatic potential, and effective potentials at the surface of a spin-polarized gas with  $\zeta=0.4$  and  $r_s=3$ . Results are for a self-consistent calculation using the RPA energy functional. The distance scale is in units of  $1/k_F=0.0827$  nm.

IID, are in close agreement with the RPA.

Figures 8 and 9 graph the spin-polarized surface solutions obtained using the RPA potential for an electron density of  $r_s=3.0$  and bulk magnetizations of  $\zeta=0.4$  and  $0.8$ . The spin densities show Friedel oscillations of wave number  $2k_{F+}$  and  $2k_{F-}$  for the spin + and - densities, respectively. In comparing the total density curves of Figs. 6, 8, and 9, the shape changes surprisingly little as a function of bulk magnetization. A similar conclusion can be drawn for the work function,

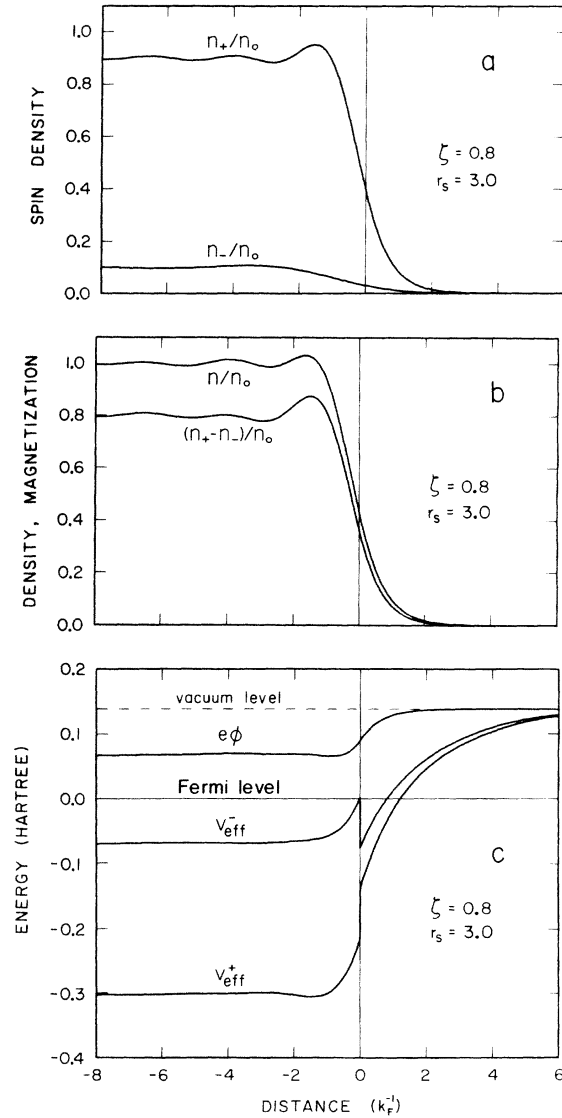


FIG. 9. Spin densities, total density, magnetization, electrostatic potential, and effective potentials at the surface of a spin-polarized gas with  $\zeta=0.8$  and  $r_s=3$ . Results are for a self-consistent calculation using the RPA energy functional. The distance scale is in units of  $1/k_F=0.0827$  nm.

which appears graphically as the difference between the vacuum level and the Fermi level and is tabulated in Table IIC. In going from  $\zeta=0$  to  $\zeta=0.8$  the effective splitting of the spin + and - bands goes from 0.0 to 6.3 eV while the work function decreases from 3.77 to 3.60 eV, a change of only 0.17 eV. Furthermore, the electrostatic potential and surface energy change relatively little with bulk magnetization. Thus, we reach the conclusion that the nonmagnetic surface properties of the model ferromagnet considered here are nearly independent of the bulk magnetization.

#### D. Application to gadolinium

We discuss the magnetization of the spin-polarized surface by applying our model to the conduction electrons of Gd. The model applies most clearly to the paramagnetic and saturated ferromagnetic states of Gd. In the paramagnetic state  $4f$  spins are randomly oriented and the average exchange field is zero. In the ferromagnetic state the  $4f$  spins are aligned, producing an exchange field which polarizes the conduction electrons. One might question whether the magnetization of  $4f$  spins is the same at the surface as in the bulk, as the model assumes. To answer this question we note that the  $4f$  spins are well represented by a Heisenberg model. While the Curie temperature of a Heisenberg thin film is generally lower than that of a solid Heisenberg ferromagnet, the saturation magnetization of even a single atomic layer is the same as for the bulk.<sup>30</sup> Thus, although the  $4f$  spins of the gadolinium surface layer may not align as quickly with decreasing temperature as those of the bulk, they probably achieve the same magnetization at absolute zero.

The density of conduction electrons of Gd corresponds to  $r_s = 2.6$ . The saturation moment is  $7.63\mu_B$  per atom,<sup>31</sup> of which  $7.0\mu_B$  is due to the seven  $4f$  electrons and  $0.63\mu_B$  results from polarization of the conduction band. Since there are three conduction electrons per atom, the relative magnetization of the conduction band is  $\zeta = 0.63/3 = 0.21$ . Rounding off the density to  $r_s = 3$  and the saturation moment to  $\zeta = 0.2$ , we assume that the first and second rows of Table IIC correspond to the paramagnetic and saturated ferromagnetic states of Gd.

The one calculated quantity which has been measured for Gd is the work function of the paramagnetic state. The calculated and measured values, 3.77 and 3.1 eV,<sup>32</sup> are in rough agreement. While no one has measured the work function of the ferromagnetic state, our calculation predicts that the result will be very nearly the same as for the paramagnetic state.

We have argued that the  $4f$  spins of the saturated

ferromagnet have the same magnetization at the surface as in the bulk. Thus, the only contribution to the surface magnetization  $M_s$  is the  $0.066\mu_B/\text{nm}^2$  associated with the conduction electrons. If we associate the entire surface magnetization with the first atomic layer of a (001) surface, it amounts to only  $0.0062\mu_B$  per atom. Thus, the total moment of a surface atom is less than a tenth of one percent larger than the total moment of a bulk atom. One concludes that, aside from the Friedel oscillations, the magnetization at the surface differs little from the bulk magnetization.

#### ACKNOWLEDGMENTS

We wish to thank A. J. Freeman of Northwestern University and David Adler of MIT for their suggestions and comments made during the course of this work.

#### APPENDIX

We outline here the numerical methods used to obtain a self-consistent solution for the spin-polarized surface problem. In general, the procedures we describe parallel those developed by Lang and Kohn<sup>1</sup> for the paramagnetic surface.

To calculate the spin densities for a given effective potential we solve the Schrödinger equation [Eq. (4.21)] for a number of  $k_x$  values between 0 and  $k_{F\sigma}$ . If the wave functions are normalized such that they approach a sine wave of unit amplitude in the bulk [Eq. (4.20)] then the spin densities can be calculated from Eq. (4.22). Integration of the Schrödinger equation for given  $k_x$  and  $\sigma$  is begun far in the vacuum where the solution is known to be a decaying exponential and proceeds into the bulk. Initially, the normalization constant is chosen arbitrarily. If integration continued far enough, the solution would become a pure sine wave from which the normalization constant and asymptotic phase could be easily determined.

Unfortunately, the accumulated error of numerical integration becomes large long before the asymptotic sinusoidal wave function is obtained. This obstacle is overcome by taking into account corrections to the sinusoidal form. To do this we note that for the sinusoidal wave function of Eq. (4.20), the asymptotic form of the spin density is

$$n_\sigma(x) \xrightarrow{x \rightarrow -\infty} n_{0\sigma} \left( 1 + \frac{3 \cos[2k_{F\sigma}x - 2\gamma_\sigma(k_{F\sigma})]}{(2k_{F\sigma}x)^2} \right) \quad (\text{A1})$$

to order  $1/x^2$ . Using these spin densities, we obtain for the effective potential

$$V_{\text{eff}}^\sigma(x) = V_{\text{eff}}^\sigma(-\infty) + (1/x^2)(C_1^\sigma \sin 2k_{F+}x + C_2^\sigma \cos 2k_{F+}x + C_3^\sigma \sin 2k_{F-}x + C_4^\sigma \cos 2k_{F-}x). \quad (\text{A2})$$

The constants  $C_1^a - C_4^a$  are determined by fitting Eq. (A2) to the given potential. By treating the  $1/x^2$  term of Eq. (A2) in perturbation theory we obtain a correction to the wave function. When the numerical wave function is fit to this corrected form, we obtain the required normalization constant and asymptotic phase.

In obtaining the corrected form for the wave function, Lang and Kohn treat the problem in first-order perturbation theory and retain the  $1/x^2$  contribution to the wave function. However, this form includes singularities in  $k_x$  at  $k_{F+}$  and  $k_{F-}$  which cannot be ignored in a spin-polarized problem. In our calculation we retain the entire first-order correction to the wave function. Our correction form, containing sine and cosine integral functions, remains finite at  $k_x = k_{F+}, k_{F-}$ . Further discussion of the analytic properties of the asymptotic wave function has been given by Feibelman.<sup>33</sup>

We now discuss the problem of obtaining a self-consistent solution. For this purpose it is useful to consider a solution in terms of the sum and difference of the spin densities,  $n = n_+ + n_-$  and  $m = n_+ - n_-$ , rather than the spin densities themselves. Given an arbitrary density and magnetization  $(n_1, m_1)$ , Eqs. (3.12), (4.21), and (4.22) allow us to compute the effective potential, wave functions, and finally a second density and magnetization  $(n_2, m_2)$ . These equations thus define two functionals  $A$  and  $B$  such that

$$n_2(x) = A[n_1, m_1; x], \quad (\text{A3})$$

$$m_2(x) = B[n_1, m_1; x]. \quad (\text{A4})$$

The self-consistent solution  $(n, m)$  is obtained when  $(n_1, m_1) = (n_2, m_2) = (n, m)$  subject to the constraint that  $n$  satisfy the charge neutrality condition, Eq. (4.4).

Since direct iteration fails to produce a self-consistent solution to the surface problem, we adopt an extension of the linear response method of Lang and Kohn. In the first step of this procedure we obtain an approximate self-consistent solution by trial and error. To do this, we first construct a trial density and magnetization  $(n_0, m_0)$ , requiring that  $n_0$  satisfy the charge neutrality condition. In practice, the trial spin densities were often taken to be of the simple form given by Eq. (4.15). We then compute  $(n_1, m_1)$  from  $(n_0, m_0)$ . Since there is no assurance that  $n_1$  will satisfy the charge neutrality condition, it is necessary

to add or subtract a small density in the surface region to obtain charge neutrality. We then compute  $(n_2, m_2)$  from  $(n_1, m_1)$ . Finally, we adjust  $(n_0, m_0)$  until  $(n_1, m_1)$  and  $(n_2, m_2)$  are in close agreement.

Having obtained two approximately self-consistent solutions,  $(n_1, m_1)$  and  $(n_2, m_2)$ , the linear response method can be used to obtain an accurate solution  $(n, m)$ . We assume that the difference between  $(n_1, m_1)$  and  $(n, m)$  can be represented by a linear combination of a limited number of appropriately chosen functions. More specifically, we assume that

$$n(x) = n_1(x) + \Delta n(x) = n_1(x) + \sum_{i=1}^N a_i U_i(x), \quad (\text{A5})$$

$$m(x) = m_1(x) + \Delta m(x) = m_1(x) + \sum_{i=1}^N b_i V_i(x), \quad (\text{A6})$$

where the  $V_i$  are harmonic oscillator functions and the  $U_i$  are the derivatives of these functions. The width and center of the harmonic oscillator functions are chosen to localize them in the surface region. The derivative functions are added to the density since they preserve charge neutrality while the harmonic oscillator functions themselves are added to the magnetization to allow adjustment of the surface magnetization. The self-consistency condition now takes the form

$$\begin{aligned} n_1(x) + \sum_{i=1}^N a_i U_i(x) \\ = n_2(x) + \sum_{i=1}^N a_i \int_{-\infty}^{\infty} dx' \frac{\delta A[n_1, m_1; x]}{\delta n_1(x')} U_i(x') \\ + \sum_{i=1}^N b_i \int_{-\infty}^{\infty} dx' \frac{\delta A[m_1, m_1; x]}{\delta m_1(x')} V_i(x'), \end{aligned} \quad (\text{A7})$$

$$\begin{aligned} m_1(x) + \sum_{i=1}^N b_i V_i(x) \\ = m_2(x) + \sum_{i=1}^N a_i \int_{-\infty}^{\infty} dx' \frac{\delta B[n_1, m_1; x]}{\delta n_1(x')} U_i(x') \\ + \sum_{i=1}^N b_i \int_{-\infty}^{\infty} dx' \frac{\delta B[m_1, m_1; x]}{\delta m_1(x')} V_i(x'). \end{aligned} \quad (\text{A8})$$

By projecting these equations onto the first  $N$  harmonic oscillator functions, we obtain a set of  $2N$  equations which may be solved for the expansion coefficients  $a_i$  and  $b_i$ . Knowing  $a_i$  and  $b_i$ , we may now compute a very nearly self-consistent result from Eqs. (A5) and (A6).

- \*Supported in part by NSF Grant No. DMR 72-3101-A02.  
 †Supported by the NSF.  
 ‡Present address.
- <sup>1</sup>N. D. Lang and W. Kohn, Phys. Rev. B 1, 4555 (1970).  
<sup>2</sup>N. D. Lang and W. Kohn, Phys. Rev. B 3, 1215 (1971).  
<sup>3</sup>P. Hohenberg and W. Kohn, Phys. Rev. 136, B864 (1964).  
<sup>4</sup>W. Kohn and L. J. Sham, Phys. Rev. 140, A1133 (1965).  
<sup>5</sup>U. von Barth and L. Hedin, J. Phys. C 5, 1629 (1972).  
<sup>6</sup>A. K. Rajagopal and J. Callaway, Phys. Rev. B 7, 1912 (1973).  
<sup>7</sup>J. A. Appelbaum and D. R. Hamann, Phys. Rev. B 6, 2166 (1972).  
<sup>8</sup>D. L. Mills, M. T. Béal-Monod, and R. A. Weiner, Phys. Rev. B 5, 4637 (1972).  
<sup>9</sup>M. T. Béal-Monod, P. Kumar, and H. Suhl, Solid State Commun. 11, 855 (1972).  
<sup>10</sup>R. A. Weiner, M. T. Béal-Monod, and D. L. Mills, Phys. Rev. B 7, 3399 (1973).  
<sup>11</sup>K. Levin, A. Liebsch, and K. H. Bennemann, Phys. Rev. B 7, 3066 (1973).  
<sup>12</sup>P. Fulde, A. Luther, and R. E. Watson, Phys. Rev. B 8, 440 (1973).  
<sup>13</sup>H. Takayama, K. Baker, and P. Fulde, Phys. Rev. B 10, 2022 (1974).  
<sup>14</sup>A. L. Fetter and J. D. Walecka, *Quantum Theory of Many-Particle Systems* (McGraw-Hill, New York, 1971).  
<sup>15</sup>F. Bloch, Z. Phys. 57, 545 (1929).  
<sup>16</sup>J. Lam, Phys. Kondens. Materie 15, 46 (1972).  
<sup>17</sup>R. L. Kautz, Ph.D. thesis (MIT, 1975) (unpublished).  
<sup>18</sup>K. S. Singwi, A. Sjolander, M. P. Tosi, and R. H. Land, Phys. Rev. B 1, 1044 (1970).  
<sup>19</sup>P. Vashishta and K. S. Singwi, Solid State Commun. 13, 901 (1973).  
<sup>20</sup>M. Rasolt and D. J. W. Geldart, Phys. Rev. Lett. 35, 1234 (1975).  
<sup>21</sup>L. Hedin and B. I. Lundquist, J. Phys. C 4, 2064 (1971).  
<sup>22</sup>C. Warner, in *Thermionic Conversion Specialists Conference, San Diego, 1971* (IEEE, New York, 1972).  
<sup>23</sup>J. R. Smith, Phys. Rev. 181, 522 (1969).  
<sup>24</sup>M. M. Pant and A. K. Rajagopal, Solid State Commun. 10, 1157 (1972).  
<sup>25</sup>H. B. Huntington, Phys. Rev. 81, 1035 (1951).  
<sup>26</sup>A. Sugiyama, J. Phys. Soc. Jpn. 15, 965 (1960).  
<sup>27</sup>J. A. Appelbaum and E. I. Blount, Phys. Rev. B 8, 483 (1973).  
<sup>28</sup>J. Vannimenus and H. F. Budd, Solid State Commun. 15, 1739 (1974).  
<sup>29</sup>S. H. Vosko, J. P. Perdew, and A. H. MacDonald, Phys. Rev. Lett. 35, 1725 (1975).  
<sup>30</sup>I. S. Jacobs and C. P. Bean, in *Magnetism*, edited by G. Rado and H. Suhl (Academic, New York, 1963), Vol. III.  
<sup>31</sup>L. W. Roeland, G. J. Cock, F. A. Muller, A. C. Moleman, R. G. Jordan, and K. A. McEwen (unpublished).  
<sup>32</sup>D. E. Eastman, Phys. Rev. B 2, 1 (1970).  
<sup>33</sup>P. J. Feibelman, Phys. Rev. B 12, 806 (1975).

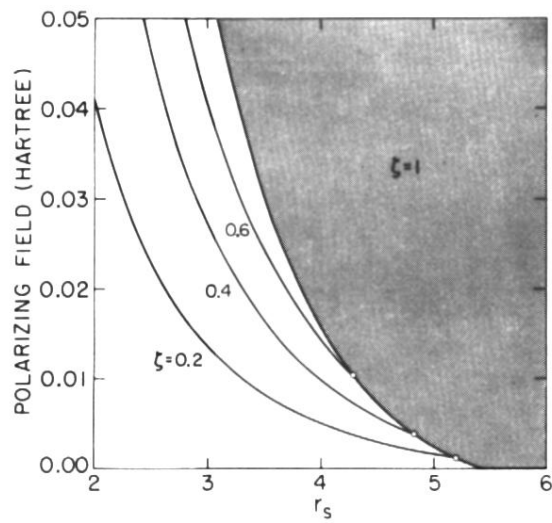


FIG. 1. Magnetic phase diagram for a HF gas. For each  $r_s < 5.45$  there is a critical field at which the relative magnetization jumps from some  $\zeta < 1$  to  $\zeta = 1$ . For  $r_s > 5.45$  the HF gas is fully magnetized even in the absence of a polarizing field. A polarizing field of 0.01 Hartree or 0.27 eV corresponds to a magnetic field of 47 million G.



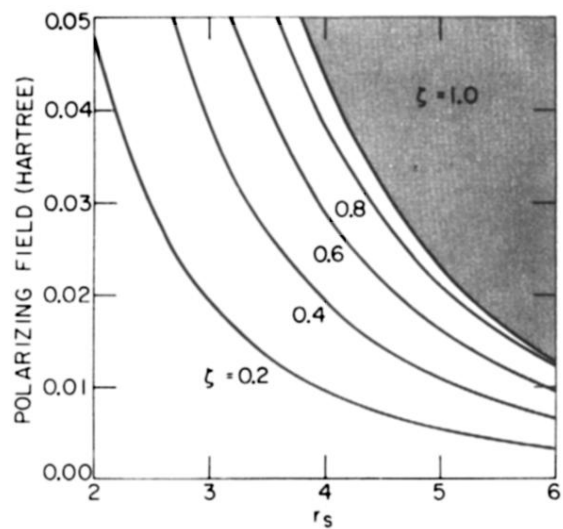


FIG. 3. Magnetic phase diagram of the RPA gas. As in the HF approximation, there is a critical field at which the relative magnetization jumps from some  $\zeta < 1$  to  $\zeta = 1$ .